The post-maximum behaviour of the changing-look Seyfert galaxy NGC 1566

V. L. Oknyansky,[1]⋆ H. Winkler,[2] S. S. Tsygankov,[3,4] V. M. Lipunov,[1,5]
E. S. Gorbovskoy,[1] F. van Wyk,[2] D. A. H. Buckley,[6] B.W. Jiang,[7,8]
N. V. Tyurina[1]

[1] *Sternberg Astronomical Institute,M. V. Lomonosov Moscow State University, 119234, Moscow, Universitetsky pr-t, 13, Russia*
[2] *Dept. Physics, University of Johannesburg, PO Box 524, 2006 Auckland Park, South Africa*
[3] *Department of Physics and Astronomy, FI-20014 University of Turku, Finland*
[4] *Space Research Institute of the Russian Academy of Sciences, Profsoyuznaya Str. 84/32, Moscow 117997, Russia*
[5] *Faculty of Physics, Moscow M.V. Lomonosov State University, Leninskie gory 1, Moscow, 119991, Russia*
[6] *The South African Astronomical Observatory, PO Box 9, 7935 Observatory, South Africa*
[7] *Key Laboratory for Particle Astrophysics, Institute of High Energy Physics, Chinese Academy of Sciences,*
19B Yuquan Road, Beijing 100049, China
[8] *School of Astronomy and Space Science, University of Chinese Academy of Sciences,*
19A Yuquan Road, Beijing 100049, China

ABSTRACT

We present results of the long-term multi-wavelength study of optical, UV and X-ray variability of the nearby changing-look (CL) Seyfert NGC 1566 observed with the *Swift* Observatory and the MASTER Global Robotic Network from 2007 to 2019. We started spectral observations with South African Astronomical Observatory 1.9-m telescope soon after the brightening was discovered in July 2018 and present here the data for the interval between Aug. 2018 to Sep. 2019. This paper concentrates on the remarkable post-maximum behaviour after July 2018 when all bands decreased with some fluctuations. We observed three significant re-brightenings in the post-maximum period during 17 Nov. 2018–10 Jan. 2019, 29 Apr.–19 Jun. 2019 and 27 Jul.–6 Aug. 2019. An X-ray flux minimum occurred in Mar. 2019. The UV minimum occurred about 3 months later. It was accompanied by a decrease of the $L_{\mathrm{uv}}/L_{\mathrm{x}}$ ratio. New post-maximum spectra covering (31 Nov. 2018 – 23 Sep. 2019) show dramatic changes compared to 2 Aug. 2018, with fading of the broad lines and [Fe X] λ6374 until Mar. 2019. These lines became somewhat brighter in Aug.-Sep. 2019. Effectively, two CL states were observed for this object: changing to type 1.2 and then returning to the low state as a type 1.8 Sy. We suggest that the changes are due mostly to fluctuations in the energy generation. The estimated Eddington ratios are about 0.055% for minimum in 2014 and 2.8% for maximum in 2018.

Key words: galaxies: active – galaxies: Seyfert – galaxies: individual: NGC 1566 – dust: extinction – X-rays: galaxies – UV

1 INTRODUCTION

Intensive study of the southern hemisphere active galactic nucleus (AGN) NGC 1566 began in the 1960s shortly after the discovery of quasars (da Silva et al. 2017; Oknyansky et al. 2019c,a; Parker et al. 2019). NGC 1566 is a nearby face-on Seyfert galaxy (de Vaucouleurs & de Vaucouleurs 1961; de Vaucouleurs 1973; Shobbrook 1966) and the nearest "changing-look" (CL) AGN (Oknyansky et al. 2018, Oknyansky et al. 2019c = Paper I). For details of the definition of CL AGNs, statistics and references see Shappee et al. (2014); MacLeod et al. (2019); Ruan et al. (2019); Runnoe et al. (2016). Because of its proximity ($D \approx 7.2$ Mpc, see comments in Paper I) NGC 1566 is one of the best objects for studying the CL phenomenon. It was one of the first known AGNs with spectral and photometric variability. Variability was discovered in 1969 by Pastoriza & Gerola (1970) when the

⋆ E-mail: oknyan@mail.ru

broad Hβ line was found to be significantly weaker than in earlier spectra from 1956 (de Vaucouleurs & de Vaucouleurs 1961) and 1962 (Shobbrook 1966). This was shortly after the discovery of variability of Seyfert galaxies (Fitch et al. 1967). During next two decades, NGC 1566 was intensively monitored (Quintana et al. 1975; Alloin et al. 1985; Winkler 1992; Baribaud et al. 1992). Quintana et al. (1975) published the first optical light curve, covering the period of 1955-1971. This correlated with the spectral variations, and they noted that NGC 1566 became a "weak Seyfert" after 1969. The object was in such low state with very weak broad permitted lines in its optical spectrum for about next 12 years (Alloin et al. 1986). Occasional brightenings of Hβ were noted in the period 1982-1991 (Alloin et al. 1985, 1986; Kriss et al. 1991; Winkler 1992; Baribaud et al. 1992), but these surges were not as strong as the outbursts of 1962 and 2018. The first photoelectric *UBV* monitoring of the object was obtained in 1974-1975 by Penfold (1979), who also collated all photometric data for 1954-1975 and confirmed that broad Hβ intensity variations correlated with optical variability. It is interesting that after the maximum of 1962 NGC 1566 had a deep minimum and then brightened again on a short time scale (months) in 1963. Such re-brightenings soon after deep minima might be a common feature of the variability of NGC 1566 and other CL AGNs. Also, if an AGN is known to be a CL AGN, then it may show dramatic variability in the future (MacLeod et al. 2019). For NGC 1566 at least two dramatic brightenings with changing looks have been observed, one in 1962 and the other in 2018. NGC 1566 was not called a "Changing Look" AGN before 2018 (Oknyansky et al. 2018) because this terminology only came into common use over the last few years.

The most intensive and longest duration previous photometric monitoring only covered the IR (*JHK*; Glass 2004). Bright states in the IR were observed in 1982 and 2000. In 1982 the stronger broad line emission was clearly seen, but no spectra were obtained in 2000. The gaps in spectral coverage were sometimes too long, meaning that possible CL episodes with dramatic spectral changes could well have been missed. It is entirely possible that high states of NGC 1566 such as in 1962 (Shobbrook 1966; Pastoriza & Gerola 1970) and 2018 (see Oknyansky et al. 2018 and Paper I) are recurrent events happening on timescales of several decades. Smaller amplitude recurrent variations on slightly shorter time-scales of < 10 years have also been suspected before (Alloin et al. 1986).

The first multi-wavelength investigations of the variability of NGC 1566 (X-ray, UV, optical and IR), as well as the first IR reverberation mapping and investigation of variability of UV/optical emission lines, were published by Baribaud et al. (1992). It is probable that the time delays (~ several months) they found are significantly overestimated (presumably because of the low cadence of the observations) and that more realistic ones are probably less than 20 days (Oknyanskij & Horne 2001). The size of the broad-line region (BLR) is typically at least a few times smaller than the distance from the central source to the inner edge of the dust torus (see e.g., Netzer 2015) and so the expected time delays in variability of broad emission lines might be just a few days.

Most subsequent studies of NGC 1566 published over the past three decades have not been investigations of spectral and photometric variability but rather of the morphology and properties of the circumnuclear environment (see e.g., da Silva et al. 2017; Combes et al. 2019) and on large scales (Elagali et al. 2019). Only recently, after the discovery of the strong outburst in the X-ray, UV, optical and IR-continua peaking in July 2018 (see details and references in Oknyansky et al. 2019c; Parker et al. 2019) has intensive multi-wavelength and spectral monitoring been initiated and the changing look in the optical spectrum revealed (Paper I and then Ochmann et al. 2020).

The spectral transition during the CL event of NGC 1566 not only manifested in dramatic intensity changes of the broad emission lines but also in strengthening of high-ionisation coronal lines such as [Fe x] λ6374. After maximum was reached in July 2018, fluxes in all bands declined, with some re-brightenings in December 2018 (Grupe et al. 2018b) and at the end of May 2019 (Grupe et al. 2019). Such post-maximum re-brightening episodes are probably typical for some fraction of CL AGNs since such events have been noted in several other CL AGNs (Oknyansky et al. 2017, 2018; Katebi et al. 2018).

In this paper we present results of the continuation of our multi-wavelength (optical, UV and X-ray) monitoring of NGC 1566 using the data obtained with *Neil Gehrels Swift Observatory* and the MASTER Global Robotic Network over the period 2007-2019 initiated by Oknyansky et al. (2019c). Preliminary results have appeared also in Oknyansky et al. (2019a). Here we provide more complete data and results and additional spectral, photometric (optical, UV) and X-ray data collected up to December 2019. We investigate in detail the post-maximum behaviour of the object and report an additional re-brightening in August 2019. We also present the analysis of our optical spectra obtained with the South African Astronomical Observatory 1.9-m telescope from Aug. 2018 to Sep. 2019.

2 OBSERVATIONS, INSTRUMENTS AND DATA REDUCTION

2.1 *Swift*: X-ray , Ultraviolet, and Optical Observations

NGC 1566 has been a regular target of observation for the *Neil Gehrels Swift Observatory* (Gehrels et al. 2004) for many years, starting in late 2007. Findings resulting from this monitoring programme have been published in a variety of studies (Kawamuro et al. 2013; Ferrigno et al. 2018; Grupe et al. 2018a,b; Oknyansky et al. 2019c; Grupe et al. 2019; Parker et al. 2019). In the present paper we have added to the analysis the most recent data (both from the XRT and UVOT telescopes), using the same methods as in Paper I and Oknyansky et al. (2017), but we uniformly re-reduced all available data to ensure usage of the most recent versions of the software and calibration files. No significant variations were found between different versions of the reduced data. The new data include 51 dates for interval from 26th Aug.2019 till 5 Dec.2019. This allows us to trace the long and shot term evolution of NGC 1566's behaviour including post maximum period.

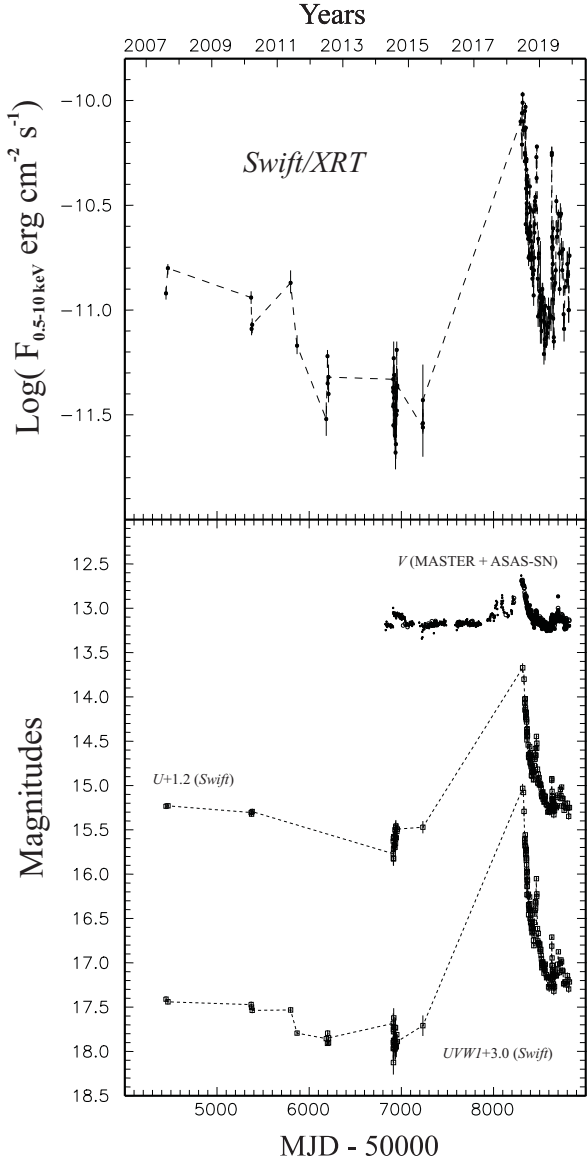The results obtained with the XRT and UVOT tele-

Figure 1. Multi-wavelength observations of NGC 1566 spanning the period 2007 Dec. 11 to 2019 Dec. 5. *Top panel:* The *Swift*/XRT 0.5–10 keV X-ray flux (in erg cm^{-2} s^{-1}). *Bottom panel:* Optical–UV photometric observations. The large open circles represent MASTER unfiltered optical photometry reduced to the *V* system while the points are *V* ASAS-SN (nightly means) reduced to the *Swift* *V* system. The filled circles show MASTER *V*-band photometry. The small open boxes correspond to the *U* and *UVW*1 *Swift*/UVOT photometry.

Figure 2. Multi-wavelength observations of NGC 1566 shown just for 2018-2019. *Top panel:* The *Swift*/XRT 0.5–10 keV X-ray flux (in erg cm^{-2} s^{-1}). *Bottom panel:* The large open circles represent MASTER unfiltered optical photometry reduced to the *V* system while the points are *V*-band ASAS-SN (nightly means) reduced to the *Swift V* system. The filled circles show MASTER *BV* photometry results. The open boxes correspond to the *UVW*1 and *UBV* data obtained by *Swift*. The arrows indicate the Events 1, 2 and 3 (see text for the details).

scopes are shown in Fig. 1–2 and will be discussed below in sections 3.1 and 3.2.

2.2 Observations with the MASTER network

Details on the MASTER (Lipunov et al. 2010), photometry methods, comparison stars, reductions and references can be found in Paper I. New observations (230 new dates) include interval after 25th Aug. 2018 till 5th Dec.2019.

The MASTER observation results are presented in Fig. 1 and 2. There we also show the ASAS-SN (All-Sky Automated Survey for Supernovae, Shappee et al. 2014;
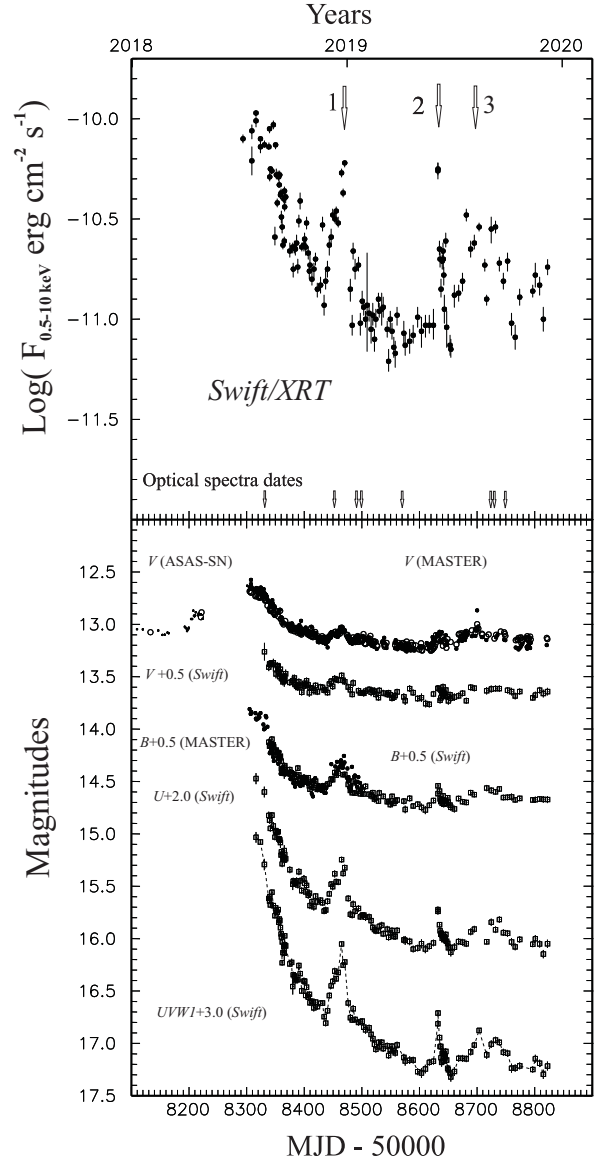
Kochanek et al. 2017; Dai et al. 2018) *V*-band magnitudes reduced to the *V* *Swift*/UVOT system. These light curves are discussed below in section 3.2.

2.3 Optical spectral observations and reductions

Low- and medium-resolution spectra of NGC 1566 were obtained on 10 nights over the period Aug 2, 2018 to Sep 23, 2019 (see Table 1) with the 1.9 m telescope at SAAO in Sutherland. The August 2 spectrum was published in Paper I. We used the SpUpNIC Cassegrain spectrograph (Crause et al. 2019) with low (300 grooves per mm) and
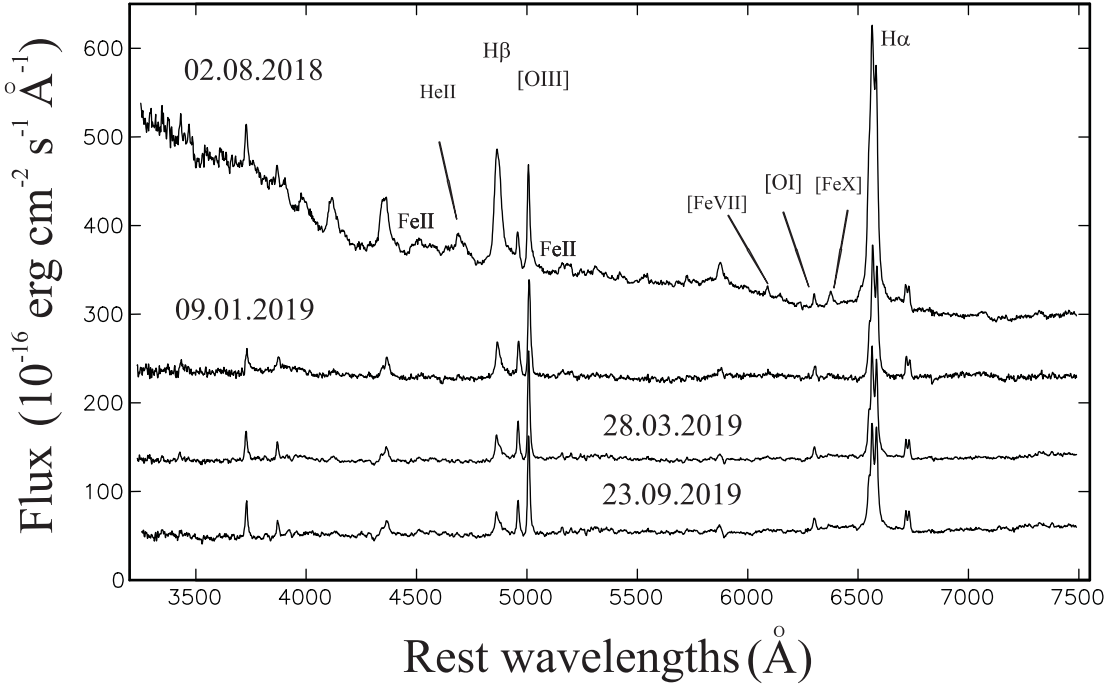
Figure 3. The isolated nuclear (low-resolution) non-stellar spectra of NGC 1566 (for 2 Aug. 2018, 9 Jan. 2019, 28 Mar. 2019 and 23 Sep. 2019) obtained by subtraction of the host galaxy spectrum from the original spectrum. Some spectra are shifted up by $2 \times F_c$ (28 Aug. 2018 and 9 Jan. 2019) and F_c (28 Mar. 2019) respectively for display purposes (where $F_c = 10^{-14}$ erg cm^{-2} s^{-1}Å^{-1}).
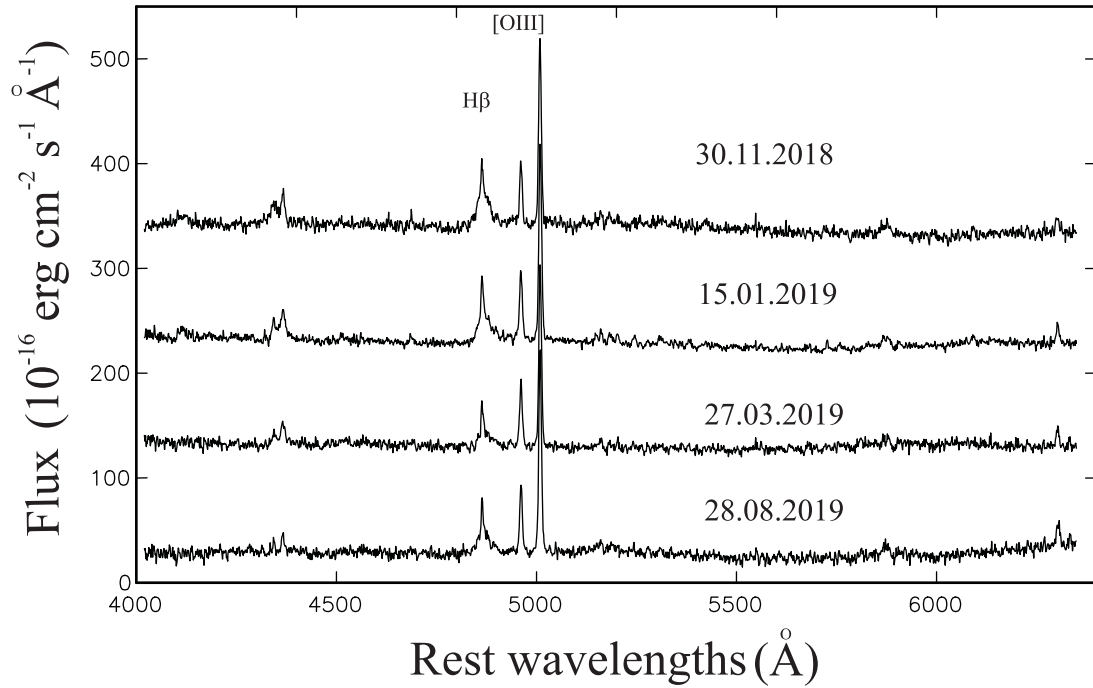

Figure 4. The isolated nuclear (medium-resolution) non-stellar spectra of NGC 1566 obtained by subtraction of the host galaxy spectrum from the original spectrum (see details in the text). Some spectra are shifted up by $3 \times F_c$ (30 Nov. 2018), $2 \times F_c$ (15 Jan. 2019) and F_c (27 Mar. 2019) respectively for display purposes (where $F_c = 10^{-14}$ erg cm^{-2} s^{-1}Å^{-1}).

Table 1. Summary of optical spectral observations.

Date	Resolution	Integration time (s)	Slit ($''$)	Flux calibration
2 Aug. 2018	low	2×600	2.7	yes
30 Nov. 2018	medium	2×600	0.9	yes
1 Dec. 2018	low	2×600	2.7	no
1 Dec. 2018	medium	2×600	0.9	yes
9 Jan. 2019	low	3×600	2.7	yes
15 Jan. 2019	medium	2×1200	0.9	yes
27 Mar. 2019	medium	2×600	0.9	yes
28 Mar. 2019	low	2×600	2.7	yes
28 Aug. 2019	medium	2×1200	0.9	yes
3 Sep. 2019	low	2×600	2.7	yes
23 Sep. 2019	low	2×600	2.7	yes

medium (500 grooves per mm) resolution gratings. The former span the range 3300 to 8500Å with a nominal resolution of about 7 Å, while the range for the latter was typically 3600 to 6400Å with a nominal resolution of about 4 Å. The spectrograph slit was oriented east-west. On each occasion at least two spectra were recorded and averaged into a single spectrum. Integration times and slit widths are given in Table 1. All spectra from Aug 2, 2018 to Sep 23, 2019 were reprocessed and measured in a uniform way. The low-resolution spectrum from Dec 1, 2018 could not be calibrated since the associated standard star observation could not be carried out. We use this spectrum just for visual analysis of emission lines.

Here we use the same methods for subtracting off-nuclear spectra as in Paper I, where details can be found. The isolated nuclear non-stellar spectra in NGC 1566 were obtained by subtraction of the background galaxy starlight, estimated by suitably scaling an off-nuclear spectrum of the same galaxy, from the spectra displayed in Fig. 3 (low resolution) and in Fig. 4 (medium). These spectra and the results will be discussed below in section 3.3.

3 RESULTS

3.1 *Swift*/XRT results

The lightcurve in the 0.5–10 keV band (spanning the time period from Dec 11, 2007 to Dec 4, 2019) is shown in Fig. 1 (top panel) and for just 2018-2019 in Fig. 2 (top panel). The variability of the source observed in 2007–2018 was discussed in Paper I. Between 2007-2015 *Swift*/XRT observations were made only a few times per year. From these we can only conclude that the X-ray flux was decreasing to the minimum in 2014–2015. After 2015 there was unfortunately a gap of about 3 years in the observations. Intensive monitoring was started in 2018 just after the discovery of the strong X-ray outburst in June 2018 (see details in Paper I). After a maximum was reached at the beginning of July 2018, the fluxes in all bands decreased significantly, but some re-brightenings were observed in MJD ranges 58440-58494 (hereafter referred to as "Event 1") and 58603-58654 ("Event 2") (Grupe et al. 2018b, 2019). One

more re-brightening ("Event 3") was observed on Aug 5, 2019 mostly from the MASTER data, but on the nearest date of X-ray observations (Aug 8) NGC 1566 was relatively bright, both in X-rays and *UVW1*. Unfortunately, observations in other UVOT bands were not made at this date.

The minimum X-ray flux level recorded during 2018-2019 of about $(6.2\pm0.1)\times 10^{-12}$ erg cm^{-2} s^{-1} was observed on Mar 3, 2019 (MJD 58546), while the most significant maximum flux measured on Jul. 16, 2018 (MJD 58316) was $(1.07\pm0.04)\times 10^{-10}$ erg cm^{-2} s^{-1} – i.e., a decline of a factor of 17. That is significant variability, but smaller than the brightening by a factor of 50 times reported in our previous paper (Paper I) from a minimum in 2014 to Jul. 2018. As can be seen from Fig. 1 and Fig. 2, after the minimum in Mar. 2019 the X-ray flux started increasing (if we remove from consideration the rapid brightenings in Event 2 and Event 3). The X-ray flux level observed on Sep 5, 2019 of $2.9\pm0.2 \times 10^{-11}$ erg cm^{-2} s^{-1} was about 4.7 times higher than it was on Mar 3, 2019. The spectral photon index remained ~1.5 between Mar. and Sep. 2019. This indicates that the X-ray spectrum had become harder than it was at its maximum flux state in Jul. 2018 when the spectral photon index reached the value of about 2.2.

Our analysis in Paper I revealed a strong dependence of the spectral photon index on the source luminosity – meaning that the amplitude of the X-ray variability was higher for soft X-rays. The strong flux decline observed during the roughly 9 months after the maximum of Jul 2018 was about 30 times in the soft band (0.5–2.0 keV) and about 20 times in the hard band (2-10 keV). So we again see that the variations are higher in soft X-rays than in hard X-rays. Meanwhile, during the slow growth from Mar. to Sep. 2019 we didn't find any significant difference in the amplitudes of soft and hard X-ray fluxes.

We estimate Eddington ratios for the minimum (2014) and maximum (2018) using the 2–10 keV fluxes and a mass of ~ $10^{6.9}$ M$_\odot$ (Woo & Urry 2002), a distance of ~7.2 Mpc and taking a bolometric correction factor of 20 (Vasudevan et al. 2009). The obtained Eddington ratios are then ~0.055% for 2014 and ~2.8% for 2018.

3.2 *Swift*/UVOT and MASTER photometry compared with *Swift*/XRT results

Light curves in the optical *VBU* and UV bands are well correlated as can be clearly seen in Fig. 1 (bottom panel) for 2007-2019 and Fig. 2 (bottom panel) for 2018–2019. The UV/Opt variation are mostly in agreement with X-ray variations for the minimum at 2014-2015 and the significant brightening to the maximum reached in July 2018. This brightening was started about 9 months before the maximum from the end of 2017 as seen in the ASAS-SN data (Dai et al. 2018; Parker et al. 2019). This was also independently confirmed by our MASTER photometry. The rise and decay times were about the same duration, viz. ~9 months. The variations between the maximum and minimum brightness during the previous year were consequently about $0.^m5$ in *V*, 1.0^m in *B*, 1.5^m in *U* and 2.5^m in *UVW1*.

These differences for the UV/Opt bands can be explained at least in part by a more significant contribution from the host galaxy at longer wavelengths. We suspect that for the 2014 minimum most of the optical and UV fluxes in

the aperture were from the host galaxy. So we can use the magnitudes at minimum light to estimate the fluxes from the host galaxy in the observed bands and to estimate partial amplitudes in each band for the nucleus during the drop from the maximum in Jul 2018 until Mar. 2019. We find that these amplitudes were similar, with variations of factors of ~ 9 times in both UV and optical (UBV) bands.

As can be seen in Fig. 1 and Fig. 2, all the variations in the optical and UV correlate well with the X-ray flux variations. After the maximum reached at the beginning of July 2018 the fluxes in all bands decreased quite rapidly, but with some fluctuations. The magnitude of the decline is largest for X-rays and decreases with increasing wavelength. There are several additional differences between X-ray and Opt/UV variability which should be noted. Firstly, day-to-day X-ray flux fluctuations were observed, on occasions with amplitudes much larger than for UV and optical rapid variations on the same time scale. The difference might be due to a much lower constant host galaxy contribution to X-rays and relatively smaller size of the X-ray emitting region. Some uncorrelated variations in X-ray and UV are present and might be connected in part with a possible small time lag, smaller than the resolution of the observations. The lags between X-ray and UV/Optical variations were found for some tens of other AGNs (Buisson et al. 2017) and usually these time delays are several times longer than what is predicted for a thin accretion disk by Shakura & Sunyaev (1973). If we take into account these results and that the lags are $\tau \sim R/c \sim \dot{m}^{1/3} M^{2/3}$, then the expected delay values for NGC 1566 can be estimated to be less than 1 day. This estimate is in agreement with our analysis of the light curves, but the details will be discussed in a future paper.

The minimum in the optical and UV bands was reached not in Mar. 2019, as for X-ray, but about 3 months later (if we do not take into account Event 2). From 3 Mar. – 16 Jun. 2019 the flux in $UVW1$ decreased by a factor of ~2 times, in U by ~1.7 and in B by ~1.2, while in V it stayed about the same. This difference could be due to variations in obscuration which have the biggest effect in the UV, and have no effect for X-ray flux, which grew during this interval. The variations of $R = L_{UV}/L_{X-ray}$ are shown in Fig. 5. The values L_{X-ray} and L_{UV} were calculated the same way as described by Ruan et al. (2019). The host-galaxy contamination to the UVW1 was also removed the same way. As can be seen from Fig. 5, the ratio R decreased significantly after Mar. 2019. A possible interpretation of this is given in the Discussion below.

The most significant re-brightening phases in the light curves (Events 1-3) seen in X-ray are also present in the UV and optical light curves. The levels of the re-brightening reached in the UV and optical bands during Event 1 are significantly higher than for Event 2 (see Fig. 6 and Fig. 7). This contrasts with the X-ray variations for which fluxes in the maxima were about the same. The X-ray and UV variations for Events 1 and 2 correlate well, but the regression lines are very different for each event (see Fig. 7) and that can reduce the correlation if the data are combined. The reason for the difference between Event 1 and Event 2 can be explained by a significantly shorter duration of X-ray outburst of Event 2 and a relatively larger size of the UV/Optical region compared to the X-ray one. Also, this difference is correlated with a decrease of the ratio R be-
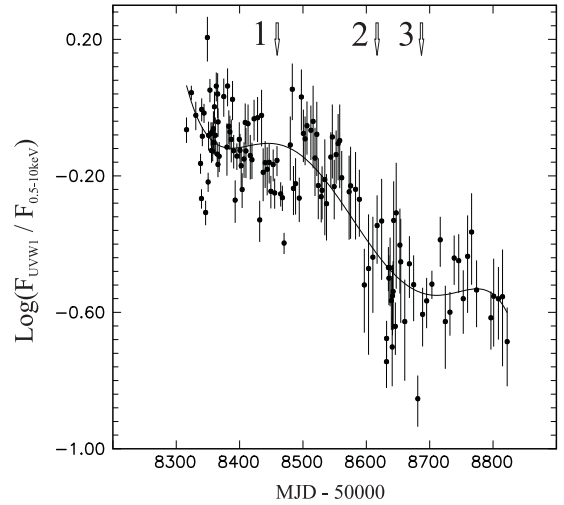

Figure 5. Variations of $F(\mathrm{UVW1})/F(\mathrm{X\text{-}ray})$ during 2018-2019. The solid line is a fifth-order polynomial approximation. The arrows indicate the Events 1, 2 and 3 (see text for more details).
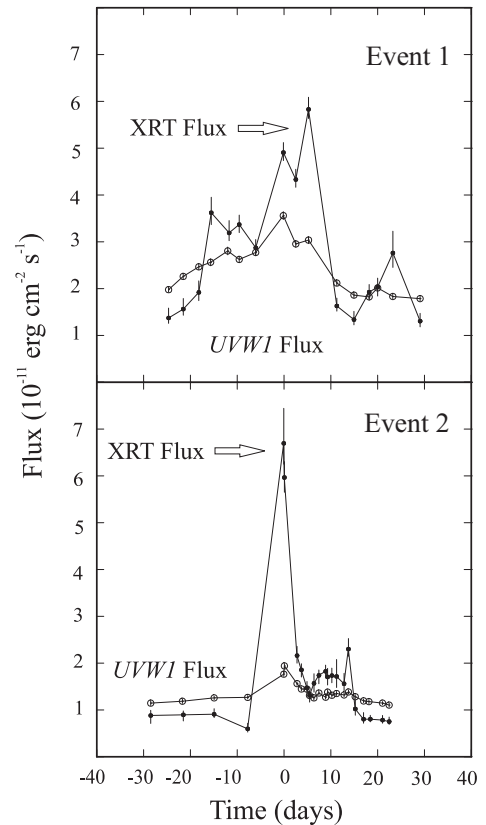

Figure 6. Light curves for $UVW1$ and XRT (in fluxes) during Event 1 and Event 2. Zero time in both cases corresponds to the maximum in the UV light curves.

tween Events 1 and 2. We do not show the relation between the X-ray and UV fluxes for Event 3 since the maximum at Aug. 5 2019 was missed by *Swift*. This event was also very short, but the amplitude in V was brighter than for Events 1 and 2.
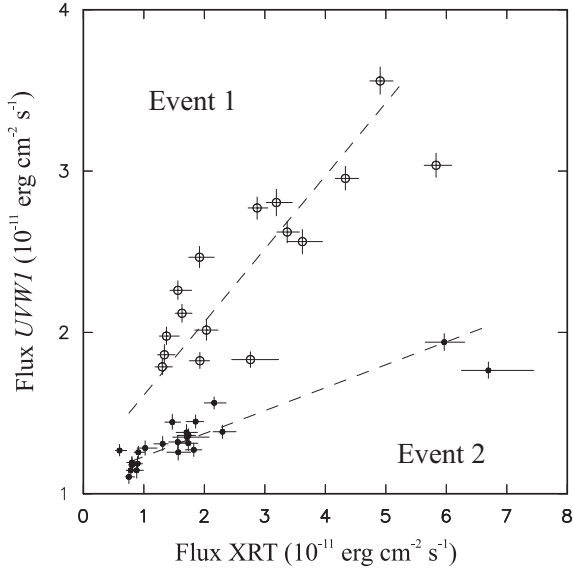
Figure 7. Comparison of the *UVW*1 flux to the XRT flux in Events 1 and 2.
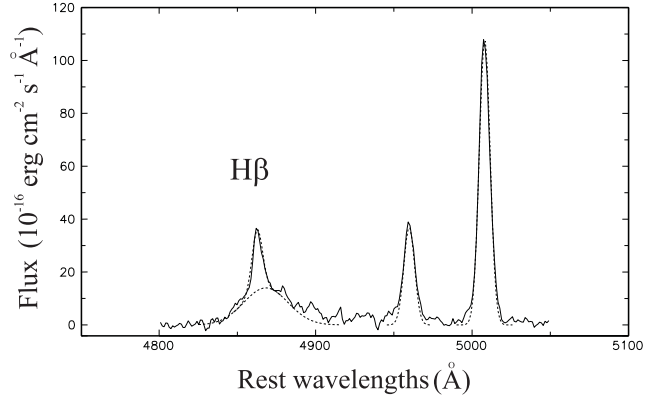

Figure 8. The nuclear spectrum of 15 Jan 2019 with the estimated continuum subtracted (solid line) in the Hβ and [O III] λ5007 region. The narrow and broad line Gaussian component fits are shown by dashed lines.

3.3 Optical spectrum: new results

In Paper I we described in detail our spectrum obtained on Aug 2, 2018, which revealed a dramatic strengthening of the broad Balmer emission lines, the Fe II emission lines, high-ionization coronal lines and the UV continuum compared to what had been published earlier. This result confirmed that NGC 1566 can be called a CL AGN. In Paper I as well as here we assume that there are no significant variations of the NLR emission lines on a time scale of 1-2 years. This assumption is usual in most publications on the spectral variability of AGNs including some CL AGNs (see e.g., Cohen et al. 1986; Shapovalova et al. 2019). To date just a few extreme events of the NLR emission lines variability were reliably proven, and these were on longer time scales (see e.g., Denney et al. 2014). Our data for NGC 1566 in this paper shows significant correlation of the permitted line variations with those of the continuum, which makes it unlikely that the relative intensity variations we highlight in this paper are connected or significantly affected by possible variability of the forbidden lines.

We have recalibrated all spectra (including data in Paper I) and remeasured relative line intensities in a uniform way. We focus here on the spectral changes since the maximum spectrum of 2 Aug. 2018. Relative line intensities are presented in the Table 2. The values listed here (noted by ∗) include the contributions of narrow components as well as blended lines: [S II] λ6716,6731, [N II] λ6584,6584 for Hα, [O III] λ4363 for Hγ, possible Fe II contamination for He II λ4686 and [O I] λ6363 with [Fe X] λ6374.

The emission from the HII region near the nucleus (da Silva et al. 2017) does not affect our analysis (see also the discussion on this point in Paper I). This can be seen when we fit multiple Gaussians to the lines (see Fig. 8). The plot shows that just one Gaussian is sufficient to fit the narrow lines, and the red-shifted HII-region component evident in the spectra shown in the da Silva et al. (2017) paper is not visible here. We further note that the broad Hβ component cannot be fitted well by a single Gaussian, which is not

unexpected given the complex broad-line profiles associated with most AGNs.

In view of the relatively low spectral resolution, and also because the broad lines are dominant, the narrow Balmer line strengths could not always be established to a reasonable accuracy. The contributions of the narrow components of the Balmer lines were therefore generated by adopting the [S II]/Hα(narrow)=0.78, [N II]λ6584/Hα(narrow)=1.18 ratios determined by da Silva et al. (2017) and [N II]λ6584/[N II]λ6548=3.07 ratio from Storey & Zeippen (2000). To get the true [Fe X]λ6374/[O I]λ6300 ratios we subtract 0.3, which is the approximate theoretical value of [O I] λ6363/[O I]λ6300 (see e.g., Storey & Zeippen 2000), from the measured values ([Fe X] λ6374+[O I] λ6363)/[O I]λ6300. As it is seen from Fig. 3, 4, 9 and Table 2, our new spectra from 30 Nov. 2018 to 23 Sep. 2019 demonstrate a dramatic dimming of the broad Balmer lines, Fe II, the UV continuum and the coronal lines Fe VII and Fe X during the ∼4 months after the maximum. Subsequently the lines were very faint during Dec. 2018-2019, although some fluctuations were noted, which probably correlated with fluctuations of the UV and X-ray fluxes. For example, the broad Balmer lines and [Fe X] line were a little bit stronger in Jan., Aug., Sep. 2019, reaching a minimum level in Mar. 2019, followed by partial re-brightenings (Event 1 and Event 3) and then a minimum level in Mar. 2019. Intensities of the Hβ, He II λ4686 and [Fe X] λ6374 lines decreased by about a factor of five between Aug. 2018 and Mar. 2019. If we take into account that there is a narrow component of Hβ, which is not variable and has an intensity about 0.16 of [O III] λ5007 (da Silva et al. 2017), then the amplitude of variability for the broad Hβ component has to be about a factor of 6-8. Some part of [Fe X] λ6374 is also radiated from a large distance from the central source (see e.g., Marco & Prieto 2005). This means that the part of the coronal line which is radiated from a smaller distance has an amplitude of variability of more than a factor of five. The Hα/Hβ ratio changed from ∼2.7 in high state (2 Aug. 2018) to ∼6.0 in the low state (28 Mar. 2019). If we take into account that this calculated value is very sensitive to the choice of narrow Hβ component, as well as to some other possible systematic
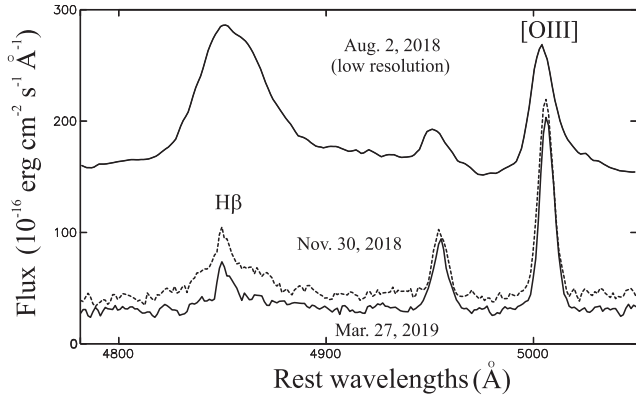
Figure 9. The isolated nuclear non-stellar spectra in NGC 1566 obtained by subtraction of the host galaxy spectrum from the original low-resolution spectrum from Aug 2, 2018 and the medium-resolution spectrum from Nov 30, 2018 (dashed line) and Mar 27, 2019 in just Hβ and [O III] λ5007 region.

errors, then the uncertainty might reach $\sim$ 30% when the AGN is in a low state. These results will be discussed below.

4 DISCUSSION

4.1 The multi-wavelength variability

Overall, the X-ray, UV/Opt variability of NGC 1566 is not unusual for a CL AGN. The dramatic changes of factors 1.5 orders of magnitude in the X-ray flux along with correlated variations at UV/Opt wavelengths is a typical property of CL AGNs. However, whilst a strong correlation of the X-ray and UV/Opt is not common among AGNs (see e.g., Edelson et al. 2000; Buisson et al. 2017), there are exceptions for some other CL AGNs, viz. NGC 2617, NGC 4151 and NGC 5548 (see e.g., Shappee et al. 2014; Oknyansky et al. 2017; Edelson et al. 2017; McHardy et al. 2014). From these results we can conclude that the variability across several wavebands in CL AGNs (spanning from X-rays to the UV/Optical) is driven by variable illumination of the accretion disc (AD) by soft X-rays. We have to determine the most significant common features of such variability. This can help us to find the most likely explanations for the CL phenomenon (see e.g. discussion and references in Paper I and below). There are several different possibilities that have been considered: variable obscuration, disk flares, tidal disruption events (TDEs), and supernova events.

The duration of the rise and decay times for the main brightening in 2018 was about the same ($\sim$ 9 months) and much longer than the recurrent brightenings (with lower amplitude) described by Alloin et al. (1986) ($\sim$20 days). A similar dramatic brightening was observed previously only in 1962, with re-brightening about one year later Quintana et al. (1975). Such re-brightenings soon after the main maximum may be common in the variability of CL AGNs.

Whilst there is good evidence for obscuration in a very high percentage of AGNs (see Gaskell 2017 and references therein), it is not the dominant variability mechanism. It is difficult to explain the dramatic rise of the X-ray and UV/optical flux by a reduction in obscuration. The main

problem with the obscuration theory is that it would predict much longer time scales for the spectral changes than what is observed in CL AGNs (see e.g., Sheng et al. 2017). For NGC 1566 we expect timescales of more than a few years for a CL event in the obscuration scenario, which is much longer than what is observed. It does not exclude the possibility of intervening clouds causing variable obscuration, but seems to exclude that as a dominant explanation for the CL mechanism. The more obvious explanation of this, and AGN variability in general, is that it is due to variation of the intrinsic energy-generation rate (for example, violent flares above the accretion disc). Since such variability is seen in all AGNs, CL AGNs are just extreme examples of this. The timescales of variability of CL-AGNs at various wavelengths are similar to the variability timescales of AGNs in general.

These two leading possibilities – intrinsic variability and variable obscuration – do not need to be mutually exclusive. For example, a dramatic change in the energy generation could cause the sublimation of dust in clouds near the central source energy source (Oknyansky et al. 2017, 2019b). If such sublimation occurs in some clouds along the line of sight, then the rise in the UV can be explained in part with the change in obscuration. The typical time for the recovery of dust clouds after the UV flux has abated can be several years (Oknyansky et al. 2017, 2019b; Kishimoto et al. 2013), but it could be less for NGC 1566 if we take into account the significantly smaller mass of the SMBH (super massive black hole) compared with NGC 4151. So we could see some increase in obscuration during the time when the energy generation is falling.

We do see some differences in variability in different wavelengths after Mar. 2019, which can be explained by variable obscuration since it must be most significant for the UV and less in optical bands, and with hardly any noticeable effect for X-ray flux. There are other possible explanations for this difference in X-ray and UV variability. For example, the strong change in the UV to X-ray flux ratio observed after Mar. 2019 can be connected with changing of the height of the X-ray source that can reduce the amount of UV/optical emission produced by reprocessing in the accretion disk (see e.g., Breedt et al. 2009). Also a transition in accretion mode might explain the observed differences in properties of variability in high and low states (see e.g., Liu et al. 2020)

The most intriguing question is what the mechanism would be for such dramatic switching on or off of the energy generation of CL AGNs. This has been explored in some firsts reports on CL events as well as in recent papers (Lyutyj et al. 1984; Penston & Perez 1984; Runnoe et al. 2016; Katebi et al. 2019). The most popular idea relates to disc instabilities. One of such mechanism of instability (Lightman & Eardley 1974) was discussed by Parker et al. (2019) in connection with NGC 1566: that the inner disk is in a low state until radiation pressure exceeds gas pressure. If that happens then an accretion disk switches on to a high state. This mechanism is consistent with the time scales of variability, but cannot explain our result that the rise time is not longer than the decay one. The radiation pressure instability in relation to NGC 1566 were also considered by Śniegowska & Czerny (2019) to explain recurrent outbursts observed in 1970-1990. This type of variability has not, however, been seen during the last 12 years. The most

Table 2. Measured emission line intensity ratios (∗ These values include the contributions of narrow components as well as blended lines. See text for the details).

Line (includes blends)	Date 02.08.18	30.11.18	01.12.2018	09.01.19	15.01.19	27.03.19	28.03.19	28.08.19	04.09.19	23.09.19
∗ Hβ/[OIII]5007	2.92	1.01	0.98	0.77	0.83	0.55	0.51	0.72	0.64	0.66
∗ [SII]/[OIII]5007	0.38	-	-	0.23	-	-	0.30	-	0.34	0.27
∗ Hα/Hβ	2.8	-	-	3.9	-	-	5.7	-	5.8	6.1
Hα/Hβ	2.6	-	-	3.7	-	-	5.5	-	5.4	6.2
∗ Hγ/Hβ	0.52	0.44	0.57	0.61	0.50	0.53	0.48	-	0.41	0.46
∗ HeII4685/Hβ	0.28	-	-	-	-	-	-	-	-	-
∗ [FeX]/[OI]6300	2.2	-	-	0.8	1.0	0.6	0.4	-	0.6	0.9
[FeX]/[OI]6300	1.9	-	-	0.5	0.7	0.3	0.1	-	0.3	0.6

significant outbursts recur in NGC 1566 on a time scale several decades (in 1962 and 2018). So we need some mechanism which can explain why the object is in a low state most of the time when the broad component of Hβ is almost undetectable but then on rare occasions we get dramatic brightenings. The idea that accretion rate transitions similar to those observed in black hole binaries may work for SMBH has previously been mooted (see e.g., Liu et al. 2020). However, the then expected time scale of several years is longer than rise and decay times observed in NGC 1566. The TDE and supernova explanations can be rejected given the differences between expected and observed time scales for such events, as well as their spectral properties and evolution. An alternative theory proposes the tidal stripping of stars (Campana et al. 2015; Ivanov & Chernyakova 2006), which could lead to more frequent and recurrent events (Komossa et al. 2017) if these stars have bound orbits similar to some known objects near the SMBH in the Milky Way. Also, these stellar striping events could trigger accretion disk instabilities and explain short time-scales for brightening, as well as why re-brightenings would recur (see e.g., Ivanov et al. 2018). However, the mechanism has not been investigated in sufficient detail yet. More references on the possible mechanisms of the CL events can be found in discussions by MacLeod et al. (2019); Runnoe et al. (2016); Ruan et al. (2019). At present we are far from understanding the CL phenomenon, and many questions remain.

4.2 The optical spectral variability

The strong variability of UV flux in NGC 1566 should affect the ionisation conditions in the emission regions near the central source and explain the strong variability of the broad emission lines. Variability of the broad Balmer and He II λ4686 lines are typical for CL AGNs. The intensities of these lines are correlated with the level of the UV/optical continuum. Possible time delays in the lines variability depend from the size of BLR. Alloin et al. (1985) and da Silva et al. (2017) estimated the size, between 1 and 15 light-days and less than 20 light-days, respectively. We do not have enough spectral epochs to perform a reverberation mapping measurement of the possible lag in Hβ variability relative to UV, but we estimate the delay as 2 days (or less) from the radius – luminosity relationship determined from other AGN

(see e.g., Shappee et al. 2014). Consistent with this model, we found that the amplitude of this variability decreases in NGC 1566 as one goes from He IIλ4686 to Hβ and Hα (see Table 2). (However we have take into account that lower amplitude of variability of Hα might in part due to blending with narrow N II lines.) Steep Balmer decrements such as the high Hα/Hβ ratio in the minimum (28 Mar. 2019) have been widely attributed to a combination of low optical depth and low ionisation parameter in the the BLR (broad line region) as in case of Mrk 609, Mrk 883 and UGC 7064 (Goodrich 1995; Rudy et al. 1988). The variability of the Balmer decrements is a typical property of a CL AGN and usually it is anti-correlated with the continuum flux variations (Shapovalova et al. 2004). For example, in the case of NGC 4151, it was measured to vary from 2 to 8 (Shapovalova et al. 2008). Variable obscuration is often considered for the explanation (see e.g, Gaskell 2017), but there are other possibilities (see e.g., Ilić et al. 2012).

One of the most interesting result found from our spectral data is the strengthening of the UV Balmer continuum during the maximum of 2018 (Paper I) and its weakness during low states. This result can be seen independently from spectra obtained by SALT in 2012 and 2018 (Ochmann et al. 2020). A similar effect has been detected in other CL AGNs as they change their states (see e.g., Shappee et al. 2014; Edelson et al. 2000), and it is probably a common property of CL AGNs.

The dramatic variability (approaching a factor of a hundred) of the soft X-ray flux in NGC 1566 has a strong effect on the ionization of gas near the central source and can thus explain the significant variability of high-ionisation lines like [Fe VII] and [Fe X] which need strong soft X-ray fluxes for such high ionisation stages. The greater variability of these coronal lines in AGN compared to the majority of other forbidden lines could be due to the transition probabilities of coronal lines being several orders of magnitude higher than for lower-ionization forbidden lines (Penston et al. 1984). This would also not be surprising since high-ionization coronal lines would be expected to arise in a smaller region than other forbidden lines (see e.g., Paper I, Rose et al. 2015; Netzer 1974; Osterbrock & Shuder 1982; Oknyanskij & Chuvaev 1982; Chuvaev & Oknyanskii 1989; Oknyanskii et al. 1991; Veilleux 1988; Landt et al. 2015a,b; Parker et al. 2016). In case of the NGC 1566 this variabil-

ity is particularly obvious (see Paper I). It might even be a typical features of CL AGNs in general. However, the interpretation of the fast variability of coronal lines presents certain difficulties. The most promising hypothesis may be an assumption about the emission of these lines in polar cones near the accretion disk (Oknyanskij 1988, 1989). If the accretion disk of NGC 1566 has an approximately face-on orientation (Grupe et al. 2019; Combes et al. 2019) the coronal regions might be extended along the line of sight. In this case the region where the coronal lines are radiated can have a large enough volume to explain observed flux in the lines and at the same time the variability can be on very small time scales and without significant lags as has been proposed for dust reprocessing by Oknyansky et al. (2015).

5 CONCLUSIONS

We have shown, from new optical spectroscopy (1.9 m SAAO) and multi-wavelength photometry (MASTER, *Swift* Ultraviolet/Optical and XRT Telescopes) of the AGN in NGC 1566, that after maximum was reached (at the beginning of July 2018) the fluxes in all bands dramatically declined with some fluctuations. Re-brightening events during the decline from maximum were observed in Dec. 2018 (Event 1), May 2019 (Event 2) and Aug. 2019 (Event 3). The amplitudes of X-ray fluxes in Event 1 and Event 2 were about the same, but UV/optical flux variations were significantly lower in the last case. The amplitude of the flux variability is strongest in the X-ray band and decreases in the UV and optical bands. We have found a strong decrease of the UV/X-ray ratio after Mar. 2019 and a rise of the|X-ray flux. The strength of the broad permitted, high ionisation [Fe x] λ6374 lines and UV continuum dropped significantly up to the end of March 2019 and NGC 1566 can , since then, again be classified as a Seyfert 1.8 to 1.9. We have therefore established that NGC 1566 is a clear case of a CL AGN. Our most recent spectra of Aug.-Sep. 2019 show lines again slightly stronger than in Mar. 2019. We suspect that the most probable scenarios of such dramatic variability are connected with AD instabilities which also can be triggered by events like stellar striping. The last option can explain recurrent CL events.

ACKNOWLEDGEMENTS

REFERENCES

Alloin D., Pelat D., Phillips M., Whittle M., 1985, ApJ, 288, 205
Alloin D., Pelat D., Phillips M. M., Fosbury R. A. E., Freeman K., 1986, ApJ, 308, 23
Baribaud T., Alloin D., Glass I., Pelat D., 1992, A&A, 256, 375
Breedt E., et al., 2009, MNRAS, 394, 427
Buisson D. J. K., Lohfink A. M., Alston W. N., Fabian A. C., 2017, MNRAS, 464, 3194
Campana S., Mainetti D., Colpi M., Lodato G., D'Avanzo P., Evans P. A., Moretti A., 2015, A&A, 581, A17
Chuvaev K. K., Oknyanskii V. L., 1989, Soviet Ast., 33, 1
Cohen R. D., Rudy R. J., Puetter R. C., Ake T. B., Foltz C. B., 1986, ApJ, 311, 135
Combes F., et al., 2019, A&A, 623, A79
Crause L. A., et al., 2019, JATIS, 5, 024007
Dai X., Stanek K. Z., Kochanek C. S., Shappee B. J., ASAS-SN Collaboration 2018, The Astronomer's Telegram, 11893
Denney K. D., et al., 2014, ApJ, 796, 134
Edelson G. S., Gedney C. J., Abbot P. A., Dyer I., Rolt K. D., 2000, Acoustical Society of America Journal, 107, 2890
Edelson R., et al., 2017, ApJ, 840, 41
Elagali A., et al., 2019, MNRAS, 487, 2797
Ferrigno C., Siegert T., Sanchez-Fernandez C., Kuulkers E., Ducci L., Savchenko V., Bozzo E., 2018, The Astronomer's Telegram, 11783
Fitch W. S., Pacholczyk A. G., Weymann R. J., 1967, ApJ, 150, L67
Gaskell C. M., 2017, MNRAS, 467, 226
Gehrels N., et al., 2004, ApJ, 611, 1005
Glass I. S., 2004, MNRAS, 350, 1049
Goodrich R. W., 1995, ApJ, 440, 141
Grupe D., Komossa S., Schartel N., 2018a, The Astronomer's Telegram, 11903
Grupe D., et al., 2018b, The Astronomer's Telegram, 12314
Grupe D., et al., 2019, The Astronomer's Telegram, 12826, 1
Ilić D., Popović L. Č., La Mura G., Ciroi S., Rafanelli P., 2012, A&A, 543, A142
Ivanov P. B., Chernyakova M. A., 2006, A&A, 448, 843
Ivanov P. B., Zhuravlev V. V., Papaloizou J. C. B., 2018, MNRAS, 481, 3470
Katebi R., et al., 2018, arXiv e-prints, p. arXiv:1811.03694
Katebi R., et al., 2019, MNRAS, 487, 4057
Kawamuro T., Ueda Y., Tazaki F., Terashima Y., 2013, ApJ, 770, 157
Kishimoto M., et al., 2013, ApJ, 775, L36
Kochanek C. S., et al., 2017, PASP, 129, 104502
Komossa S., et al., 2017, in Gomboc A., ed., IAU Symposium Vol. 324, New Frontiers in Black Hole Astrophysics. pp 168–171
Kriss G. A., Hartig G. F., Armus L., Blair W. P., Caganoff S., Dressel L., 1991, ApJ, 377, L13
Landt H., Ward M. J., Steenbrugge K. C., Ferland G. J., 2015a, MNRAS, 449, 3795
Landt H., Ward M. J., Steenbrugge K. C., Ferland G. J., 2015b, MNRAS, 454, 3688
Lightman A. P., Eardley D. M., 1974, ApJ, 187, L1
Lipunov V., et al., 2010, Adv. Astron., 2010, 349171
Liu Z., Liu H.-Y., Cheng H., Qiao E., Yuan W., 2020, MNRAS, 492, 2335
Lyutyj V. M., Oknyanskij V. L., Chuvaev K. K., 1984, Soviet Astronomy Letters, 10, 335
MacLeod C. L., et al., 2019, ApJ, 874, 8
Marco O., Prieto A., 2005, in Brandner W., Kasper M. E., eds, Science with Adaptive Optics. Springer Berlin Heidelberg, Berlin, Heidelberg, pp 315–320
McHardy I. M., et al., 2014, MNRAS, 444, 1469
Netzer H., 1974, MNRAS, 169, 579
Netzer H., 2015, ARA&A, 53, 365

Ochmann M. W., Kollatschny W., Zetzl M., 2020, Contributions of the Astronomical Observatory Skalnate Pleso, 50, 318

Oknyanskii V. L., Lyutyi V. M., Chuvaev K. K., 1991, Soviet Astronomy Letters, 17, 100

Oknyanskij V. L., 1988, Peremennye Zvezdy, 22, 956

Oknyanskij V. L., 1989, Soobshcheniya Spetsial'noj Astrofizicheskoj Observatorii, 61, 70

Oknyanskij V. L., Chuvaev K. K., 1982, Astronomicheskij Tsirkulyar, 1228, 1

Oknyanskij V. L., Horne K., 2001, in Peterson B. M., Pogge R. W., Polidan R. S., eds, Astronomical Society of the Pacific Conference Series Vol. 224, Probing the Physics of Active Galactic Nuclei. p. 149

Oknyansky V. L., Gaskell C. M., Shimanovskaya E. V., 2015, Odessa Astronomical Publications, 28, 175

Oknyansky V. L., et al., 2017, MNRAS, 467, 1496

Oknyansky V. L., Lipunov V. M., Gorbovskoy E. S., Winkler H., van Wyk F., Tsygankov S., Buckley D. A. H., 2018, The Astronomer's Telegram, 11915

Oknyansky V. L., Winkler H., Tsygankov S. S., Lipunov V. M., Gorbovskoy E. S., van Wyk F., Buckley D. A. H., Tyurina N. V., 2019a, Odessa Astronomical Publications, 32, 75

Oknyansky V. L., Shenavrin V. I., Metlova N. V., Gaskell C. M., 2019b, Astronomy Letters, 45, 197

Oknyansky V. L., Winkler H., Tsygankov S. S., Lipunov V. M., Gorbovskoy E. S., van Wyk F., Buckley D. A. H., Tyurina N. V., 2019c, MNRAS, 483, 558

Osterbrock D. E., Shuder J. M., 1982, ApJS, 49, 149

Parker M. L., et al., 2016, MNRAS, 461, 1927

Parker M. L., et al., 2019, MNRAS, 483, L88

Pastoriza M., Gerola H., 1970, Astrophys. Lett., 6, 155

Penfold J. E., 1979, MNRAS, 186, 297

Penston M. V., Perez E., 1984, MNRAS, 211, 33P

Penston M. V., Fosbury R. A. E., Boksenberg A., Ward M. J., Wilson A. S., 1984, MNRAS, 208, 347

Quintana H., Kaufmann P., Sasic J. L., 1975, MNRAS, 173, 57P

Rose M., Elvis M., Tadhunter C. N., 2015, MNRAS, 448, 2900

Ruan J. J., Anderson S. F., Eracleous M., Green P. J., Haggard D., MacLeod C. L., Runnoe J. C., Sobolewska M. A., 2019, arXiv e-prints, p. arXiv:1909.04676

Rudy R. J., Cohen R. D., Ake T. B., 1988, ApJ, 332, 172

Runnoe J. C., et al., 2016, MNRAS, 455, 1691

Shakura N. I., Sunyaev R. A., 1973, A&A, 500, 33

Shapovalova A. I., et al., 2004, A&A, 422, 925

Shapovalova A. I., et al., 2008, A&A, 486, 99

Shapovalova A. I., et al., 2019, MNRAS, 485, 4790

Shappee B. J., et al., 2014, ApJ, 788, 48

Sheng Z., Wang T., Jiang N., Yang C., Yan L., Dou L., Peng B., 2017, ApJ, 846, L7

Shobbrook R. R., 1966, MNRAS, 131, 365

Śniegowska M., Czerny B., 2019, arXiv e-prints, p. arXiv:1904.06767

Storey P. J., Zeippen C. J., 2000, MNRAS, 312, 813

Vasudevan R. V., Mushotzky R. F., Winter L. M., Fabian A. C., 2009, MNRAS, 399, 1553

Veilleux S., 1988, AJ, 95, 1695

Winkler H., 1992, MNRAS, 257, 677

Woo J.-H., Urry C. M., 2002, ApJ, 579, 530

da Silva P., Steiner J. E., Menezes R. B., 2017, MNRAS, 470, 3850

de Vaucouleurs G., 1973, ApJ, 181, 31

de Vaucouleurs G., de Vaucouleurs A., 1961, Mem. RAS, 68, 69

This paper has been typeset from a TeX/LaTeX file prepared by the author.